Acoustic Interaction Between a Coated Microbubble and a Rigid Boundary

K. Efthymiou & N. Pelekasis

Laboratory of Fluid Mechanics and Turbomachinery

Department of Mechanical Engineering

University of Thessaly, Volos, GREECE

Funding: "HERACLITUS II" Program, Greek Ministry of Education

European Union
European Social Fund

OPERATIONAL PROGRAMME
EDUCATION AND LIFELONG LEARNING
investing in knowledge society
MINISTRY OF EDUCATION & RELIGIOUS AFFAIRS
MANAGING AUTHORITY

NSRF 2007-2013
programme for development
EUROPEAN SOCIAL FUND

Co-financed by Greece and the European Union

8th GRACM International Congress, Volos, Greece, 12-15 July 2015

Microbubbles (Contrast Agents)

- Bubbles surrounded by an elastic membrane for stability
- Low density internal gas that is soluble in blood
- Diameter from 1 to 10 μm
- Polymer, lipid or protein (e.g. albumin) monolayer shell of thickness from 1 to 30 nm

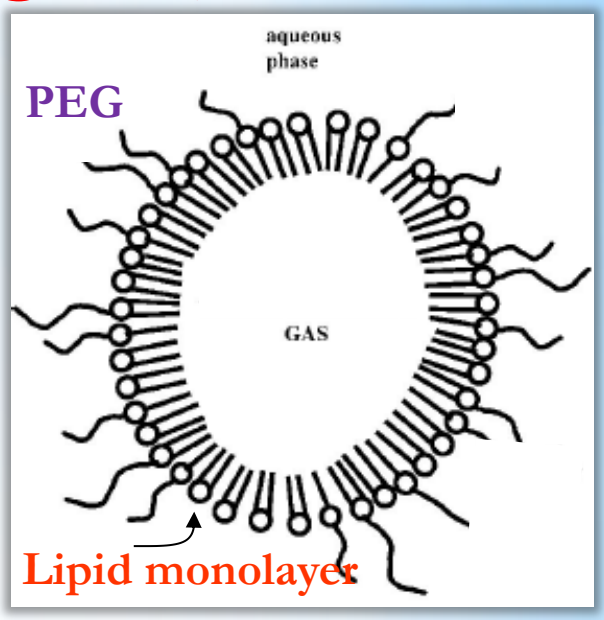

Motivation

- Contrast perfusion imaging ⇒ check the circulatory system by means of contrast enhancers in the presence of ultrasound
  (Sboros et al. 2002, Frinking & de Jong, Postema et al., Ultrasound Med. Bio. 1998, 2004)
- Sonoporation ⇒ reinforcement of drug delivery to nearby cells that stretch open by oscillating contrast agents
  (Marmottant & Hilgenfeldt, Nature 2003)
- Micro-bubbles act as vectors for drug or gene delivery to targeted cells
  (Klibanov et al., adv. Drug Delivery Rev., 1999, Ferrara et al. Annu. Rev. Biomed., 2007)

Asymmetric oscillations of a microbubble near a wall

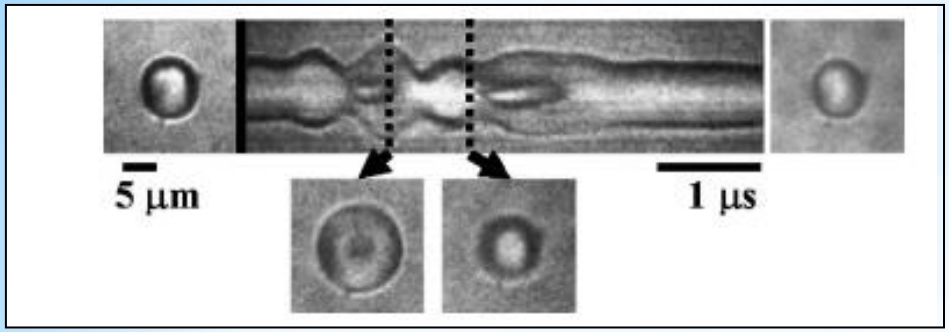

(S. Zhao et al., Applied Physics, 2005)

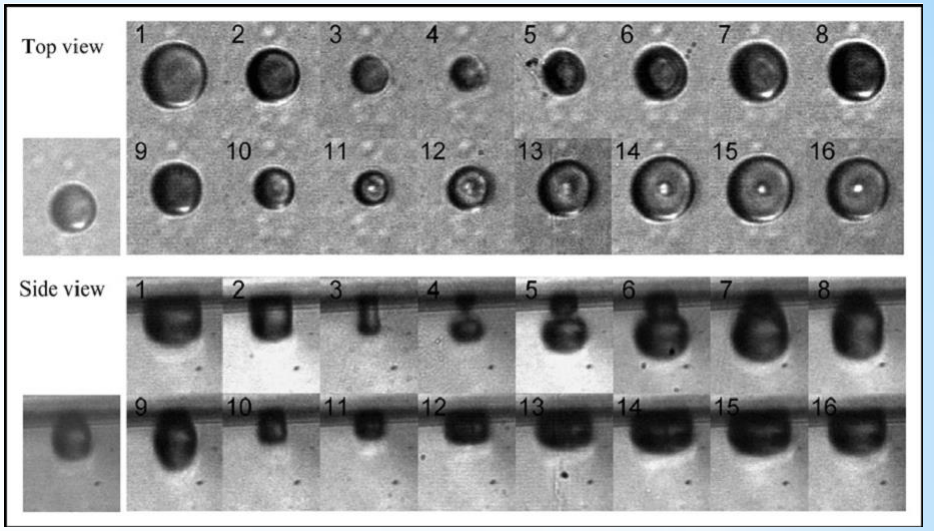

(H. J. Vos et al., Ultrasound in Med. & Biol., 2008)

- Experiments have shown that the presence of a nearby wall affects the bubble's oscillations
- Asymmetric oscillations, toroidal bubble shapes during jet inception have been observed
- The bubble oscillates asymmetrically in the plane normal to the wall, while it oscillates symmetrically in the plane parallel to the wall (i.e. deformation has an orientation perpendicular to the wall)

Controlled and Directed Local Release from Drug-loaded Microbubbles for Sonothrombolytic Therapy

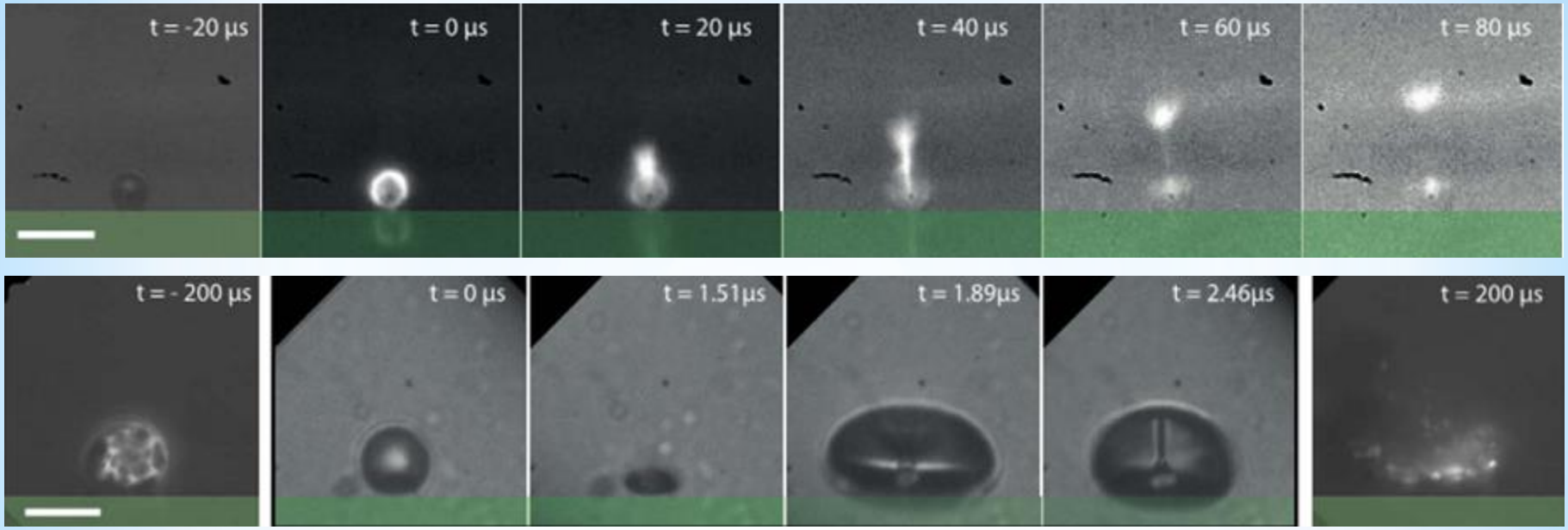

(G. Lajoinie et al., 20th ESUCI, 2015)

- **There are two regimes with different release mechanisms:**

- **Smaller microbubbles (up to 5 µm) generate a strong acoustic streaming field and a local recirculation of the flow which promotes flashing away of deactivated reagents and mixing in freshly released model drug**

- **For larger bubbles, it has been observed a quasi-systematic formation of a high-speed jet toward the substrate and the load of the microbubble is directly deposited on the membrane, which is expected to promote a highly localized clot dissolution efficacy**

Axisymmetric Pulsations

$$P'_{\infty}(t') = P'_{st}\left[1+\varepsilon\sin\left(\omega_f t'\right)\right],\quad \omega_f = 2\pi\nu_f$$

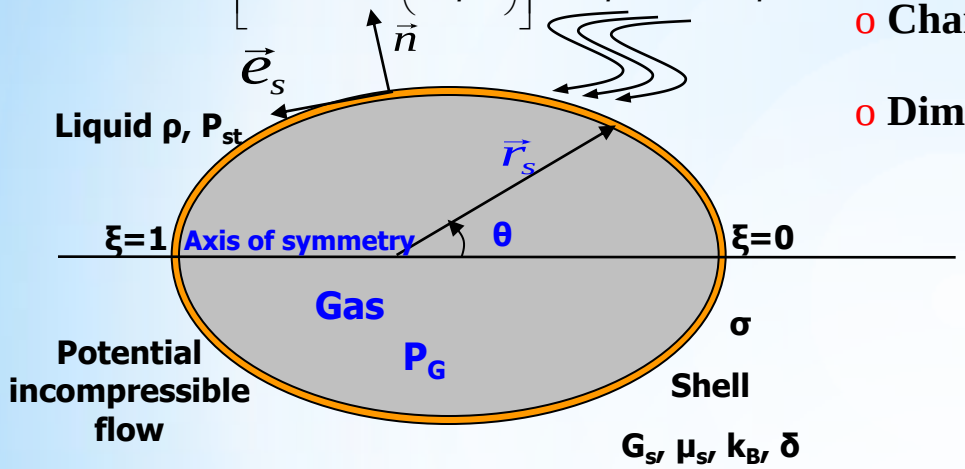

$G_{S,2d}=\delta G_S$

- Characteristic space and time scales: $R_{Eq},\ \sqrt{\rho R_{Eq}^3 / G_{S,2d}}$
- Dimensionless parameters:

$$\omega_f = \frac{\omega'_f}{\sqrt{G_{S,2d}/\left(\rho R_{Eq}^3\right)}} \qquad P = \frac{P_{St}}{\rho G_{S,2d}^2 / R_{Eq}^2}, \qquad We = \frac{G_{S,2d}}{\sigma}$$

$$\mathrm{Re}_l = \sqrt{\frac{\rho G_{S,2d} R_{Eq}}{\mu_l^2}} \qquad B = \frac{k_B}{G_{S,2d} R_{Eq}^2} \qquad \mathrm{Re}_s = \sqrt{\frac{\rho G_{S,2d} R_{Eq}^3}{\mu_S^2}}$$

- Axisymmetry
- Ideal, irrotational flow of high Reynolds number
- Incompressible surrounding fluid with a sinusoidal pressure change in the far field
- Ideal gas in the microbubble undergoing adiabatic pulsations
- Very thin viscoelastic shell whose behavior is characterized by the constitutive law (e.g. Hooke, Mooney-Rivlin or Skalak)
- The shell exhibits bending modulus that determines bending stresses along with curvature variations
- Shell parameters: area dilatation modulus $\chi=3G_s\delta$, dilatational viscosity μ_s, degree of softness b for strain softening shells or area compressibility C for strain hardening ones and the bending modulus k_B

- **Shell viscosity dominates liquid viscosity, $Re_s << Re_l$ and we can drop viscous stresses on the liquid side**
- **Therefore the tangential force balance is satisfied on the shell with the viscous and elastic stresses in the shell balancing each other**

❖ **Force balance on the bubble's interface:**

$$\vec{r} = \vec{r}_s : \left(-P_L \underline{\underline{I}} + \frac{1}{\mathrm{Re}_L} \underline{\underline{X}} \right) \cdot \vec{n} + P_G \vec{n} = \frac{2k_m}{We} \vec{n} + \overrightarrow{\Delta F} = \frac{\left(\vec{\nabla}_s \cdot \vec{n} \right) \vec{n}}{We} + \overrightarrow{\Delta F},$$

$$\overrightarrow{\Delta F} = \Delta F_n \vec{n} + \Delta F_t \vec{e}_s = -\vec{\nabla}_s \cdot \underline{\underline{T}}, \quad \underline{\underline{T}} = \underline{\underline{\tau}}_{El} + \vec{q}\vec{n} + \underline{\underline{\tau}}_{Vis}$$

$\vec{\nabla}_s$: **Surface gradient,** $\underline{\underline{T}}$: **Stress tensor**

$\underline{\underline{\tau}}_{El}$, $\underline{\underline{\tau}}_{vis}$: **Elastic and viscous stress tensors**

$\vec{q}\vec{n}$: **Transverse shear tensor due to bending moments**

❖ **Torque balance on the bubble's interface:**

$\vec{\mathbf{q}} = \vec{\nabla}_s \cdot \underline{\underline{\mathbf{m}}} \cdot (\underline{\underline{\mathbf{I}}} - \vec{\mathbf{n}}\vec{\mathbf{n}})$, $\underline{\underline{\mathbf{m}}}$: **Tensor of bending moments**

Shell Constitutive Laws – Isotropic Tension

- **Linear behavior ⇒ Hooke's law**
  Kelvin–Voigt law with viscous stresses:

$$T_1^H = G_S \frac{1+\nu_s}{1-\nu_s}\left[\lambda^2 - 1\right] = K\left(\lambda^2 - 1\right) = K\frac{\Delta A}{A}$$

K: area dilatation modulus
G_s: shear modulus
ν_s: surface Poisson ratio
$\Delta A/A$: relative area change

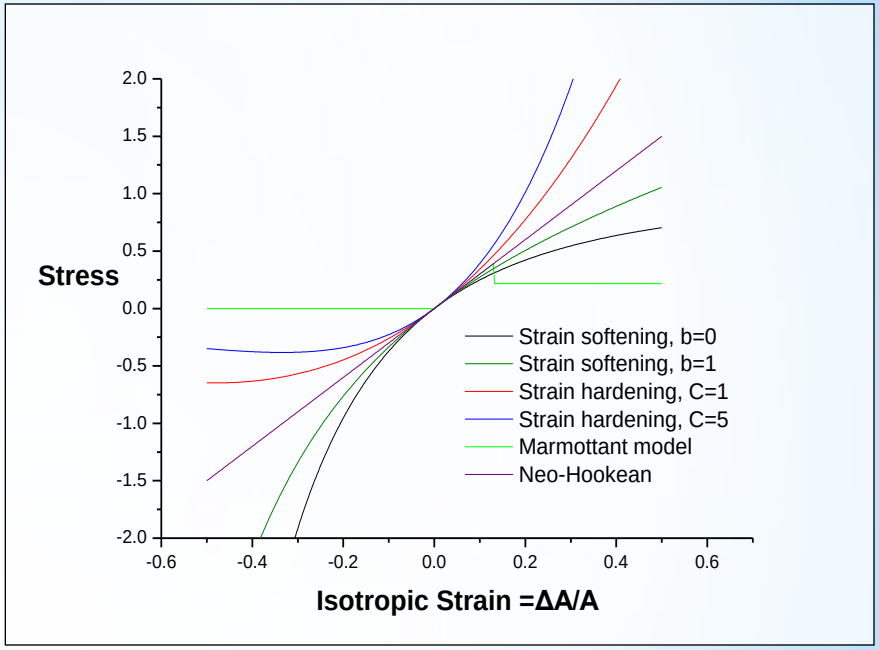

- **Strain softening material (e.g. lipid monolayer)**
  2D Mooney–Rivlin law:

$$T_1^{MR} = \frac{G_{MR}\left(\lambda^4 + \lambda^2 + 1\right)}{\lambda^6}\left[\lambda^2 - 1\right]\left[\Psi + \lambda^2\left(1-\Psi\right)\right], \quad 0 \le \Psi \le 1$$

Ψ=1-b : degree of smoothness

- **Strain hardening material (e.g. red blood-cell membrane that consist of a lipid bilayer)**
  Skalak law:

$$T_1^{SK} = G_{SK}\left[\lambda^2 - 1\right]\left[1 + C\lambda^2\left(1+\lambda^2\right)\right], \quad 1 \le C,$$

C: degree of area compressibility

Axisymmetric pulsations of a bubble near a boundary

Governing Equations

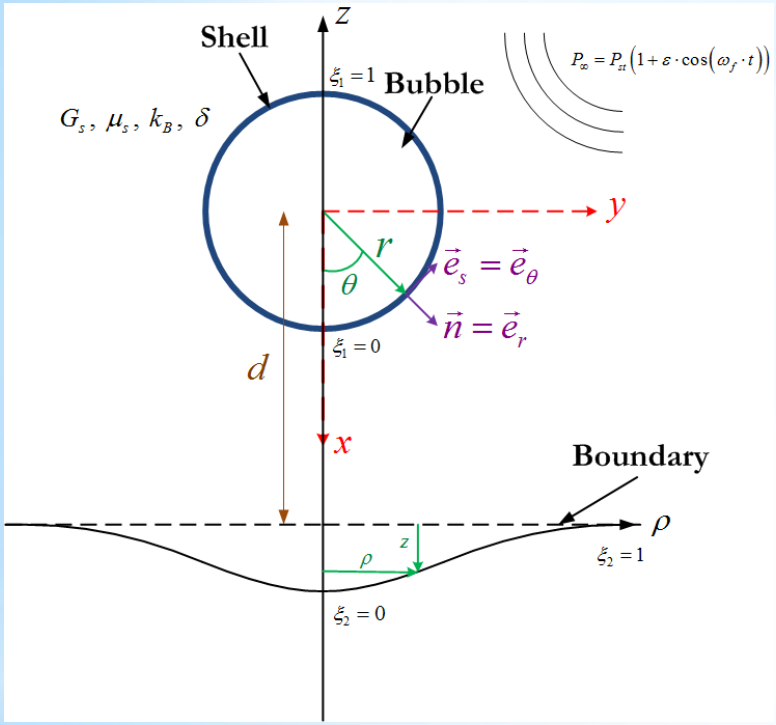

Kinematic condition of the bubble's interface in r-direction:

$$\left.\frac{dr}{dt}\right|_{r_0,\theta_0} = \frac{\Phi_\xi\cdot r_\xi + \dfrac{\partial\Phi}{\partial n}\cdot r\cdot\theta_\xi\cdot\sqrt{r_\xi^2 + r^2\cdot\theta_\xi^2}}{r_\xi^2 + r^2\cdot\theta_\xi^2}$$

Tangential force balance on the bubble's interface:

$$\frac{\partial\tau_{ss}}{\partial s} + \frac{1}{\sigma}\cdot\frac{\partial\sigma}{\partial s}\left(\tau_{ss} - \tau_{\varphi\varphi}\right) + k_s\cdot q = 0$$

Dynamic condition on the bubble's interface:

$$\frac{D\Phi}{Dt} = \frac{1}{2}\left[\left(\frac{\partial\Phi}{\partial n}\right)^2 + \frac{\Phi_\xi^2}{r_\xi^2 + r^2\theta_\xi^2}\right] + P_\infty - P_G + \frac{2k_m}{We} + \Delta F_n, \qquad k_m = \vec{\nabla}_s\cdot\vec{n}$$

Boundary conditions due to axisymmetry:

$$\frac{\partial r}{\partial\xi} = \frac{\partial\Phi}{\partial\xi} = \frac{\partial^2\Phi}{\partial\xi\partial n} = \frac{\partial^2\theta}{\partial\xi^2} = 0 \qquad \text{στο } \xi_1 = 0,\ 1 \ \ (\text{i.e. } \theta = 0,\ \pi)$$

Boundary integral equation of the interfaces:

$$\Phi\left(r_0,z_0,t\right) = \int_{S_b}\frac{\partial\Phi}{\partial n}\left(r,z,t\right)G\left(r_0,z_0,r,z\right)dS_b - \int_{S_b}\left[\Phi\left(r,z,t\right) - \Phi\left(r_0,z_0,t\right)\right]\frac{\partial G}{\partial n}\left(r_0,z_0,r,z\right)dS_b +$$

$$+\int_{S_w}\frac{\partial\Phi}{\partial n}\left(r,z,t\right)G\left(r_0,z_0,r,z\right)dS_w - \int_{S_w}\Phi\left(r,z,t\right)\frac{\partial G}{\partial n}\left(r_0,z_0,r,z\right)dS_w$$

Boundary/finite element formulation treating the boundary as a rigid wall

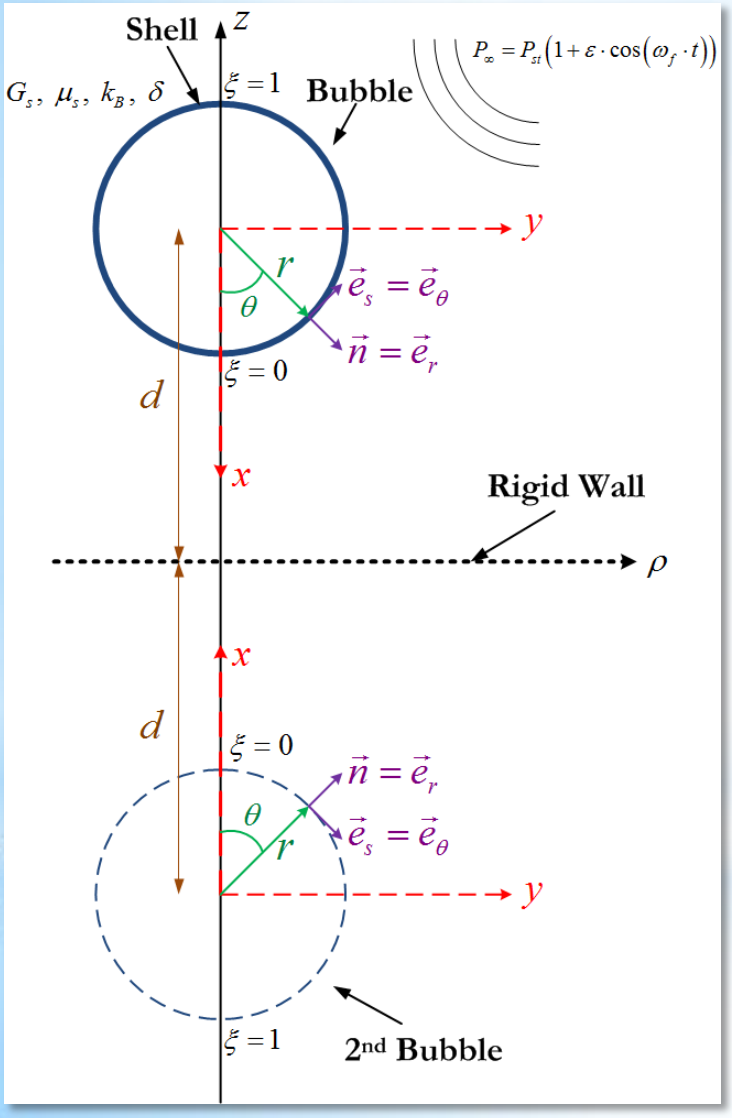

In this case a second symmetric bubble with respect to r-axis is considered

We discretize the kinematic condition, the tangential force balance and the dynamic condition by means of Finite Element Method in order to compute the position of bubble's interface and the velocity potential. Owing to symmetry, we solve only for the first bubble.

We discretize the boundary integral equation by means of Boundary Element Method in order to compute the normal velocity of the interfaces:

$$\Phi\left(r_0,z_0,t\right) = \int_{S_{b1}} \frac{\partial\Phi}{\partial n}\left(r,z,t\right)G\left(r_0,z_0,r,z\right)dS_{b1} -$$

$$-\int_{S_{b1}}\left[\Phi\left(r,z,t\right)-\Phi\left(r_0,z_0,t\right)\right]\frac{\partial G}{\partial n}\left(r_0,z_0,r,z\right)dS_{b1} +$$

$$+\int_{S_{b2}} \frac{\partial\Phi}{\partial n}\left(r,z,t\right)G\left(r_0,z_0,r,z\right)dS_{b2} - \int_{S_{b2}} \Phi\left(r,z,t\right)\frac{\partial G}{\partial n}\left(r_0,z_0,r,z\right)dS_{b2}$$

where (r_0,z_0): the field point

Integration in time of the kinematic and dynamic interfacial conditions is performed via 4th order explicit Runge – Kutta method

Filtering

- The above equations involve evaluation of spatial derivatives of third order. Consequently as the simulation proceeds short wave instabilities arise, whose wavelength is on the order of minimum element size. These instabilities cannot be eliminated by mesh refinement alone
- In order to circumvent this problem filtering of the higher modes is implemented, while monitoring the energy of the system so that it is dissipated appropriately
- The r-coordinate, the velocity potential and the flux are recalculated via the expression:

$f = \sum_{n=0}^{\infty} c_n \cdot P_n$, where P_n: Legendre polynomials and $c_n = \frac{2n+1}{2} \int_0^{\pi} f(\theta) \cdot P_n(\theta) \cdot \sin\theta d\theta$

using the first fifty terms

Benchmark

The case of saturated pulsations of an oscillating microbubble at an infinite distance from a rigid boundary is retrieved using the above technic of filtering (K. Tsiglifis & N. Pelekasis, 2013)

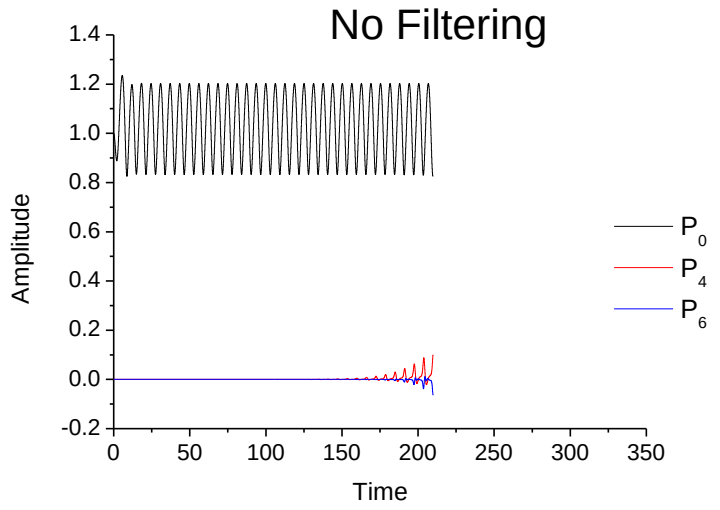

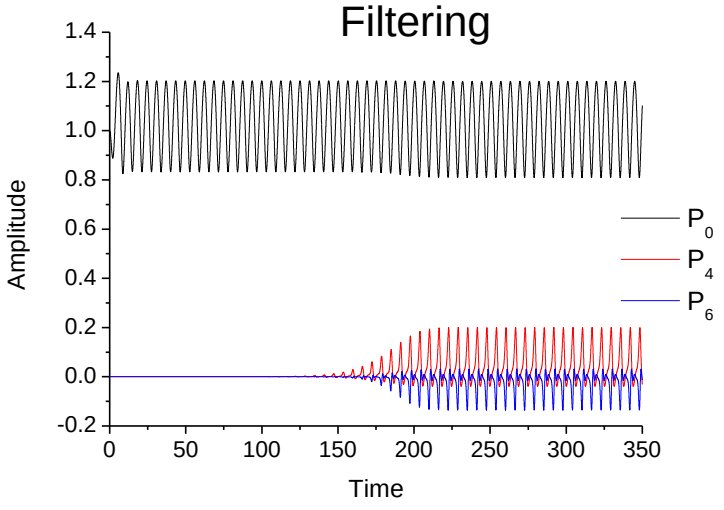

Numerical Results

Step change in pressure field: $P_\infty(t) = P_{st} \cdot (1+\varepsilon)$

Uncoated microbubble

$R_0 = 3.6\ \mu m,\ \sigma = 0.075\ {}^{N}\!/_{m},\ \nu_0 = 3622.9\ Hz,$

$\nu_f = 5553.67\ Hz,\ \gamma = 1.4,\ P_{st} = 101325\ Pa,\ \mu_l = 0$

Coated microbubble

$R_0 = 3.6\ \mu m,\ \mu_s = 20\ Pa \cdot s,\ G_{3D} = 80\ MPa,$

$\sigma = 0.051\ {}^{N}\!/_{m},\ k_B = 3 \cdot 10^{-14}\ N \cdot m,\ b = 0$ (MR shell),

$\nu_0 = 1\ MHz,\ \gamma = 1.07,\ P_{st} = 101325\ Pa,\ \mu_l = 0,\ \delta = 1\ nm$

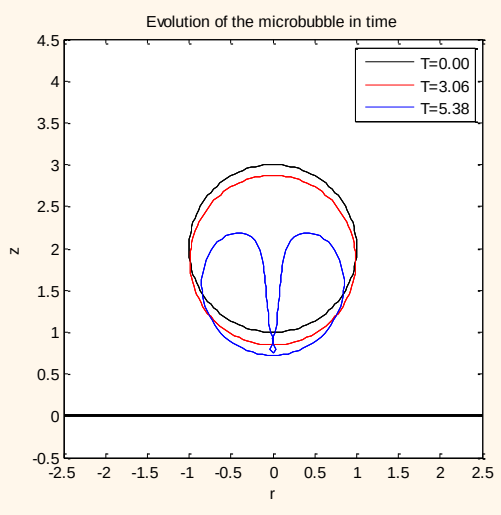

$\varepsilon = 2,\ d = 1$

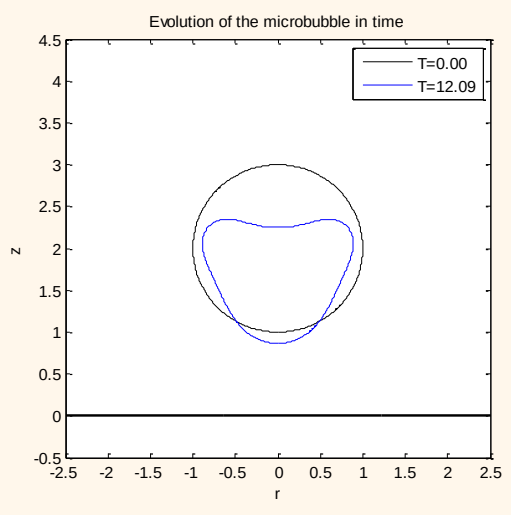

- **In both cases the microbubble approaches the rigid boundary due to the interaction with the rigid wall (secondary Bjerknes force)**
- **The uncoated bubble oscillates with its eigenfrequency ω_0 while the oscillations of the coated one are dumped due to dilatational viscosity of the shell**
- **In the case of uncoated microbubble a formation of a liquid jet in its aft region is observed while in the coated one jet formation is suppressed due to the presence of the viscoelastic shell**

Sinusoidal change in pressure field: $P_\infty(t) = P_{st} \cdot (1 + \varepsilon \cdot \cos t)$

Uncoated microbubble $\varepsilon = 2,\ d = 1$ **Coated microbubble**

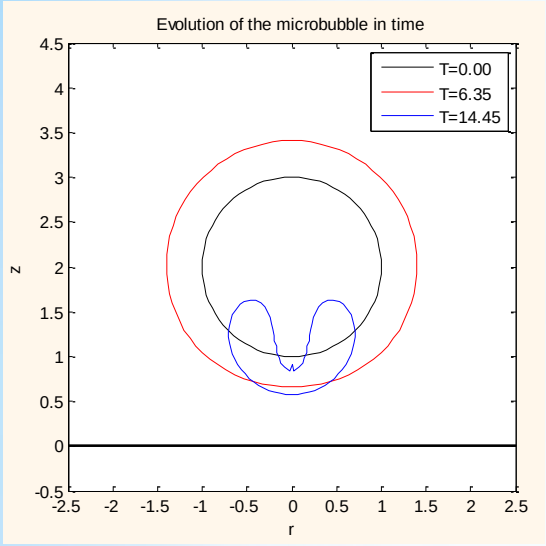

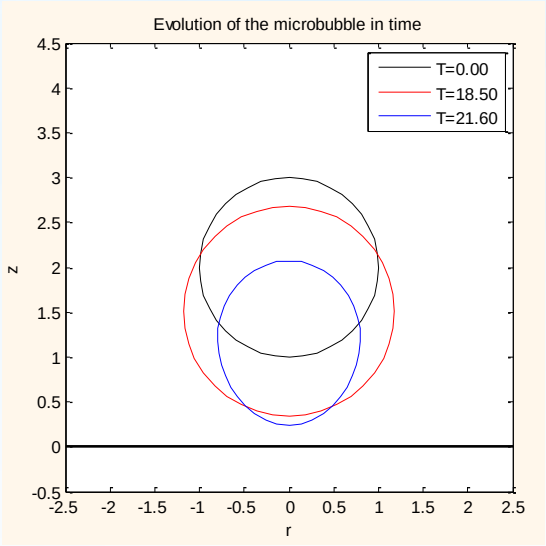

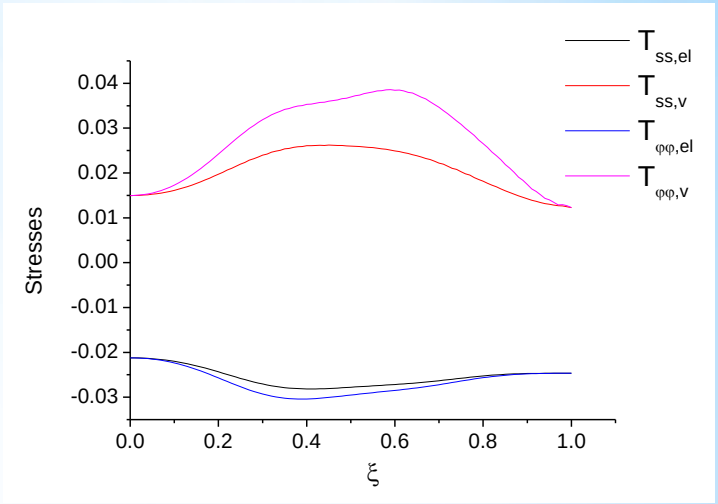

- **Also, in this case, the microbubble approaches the rigid boundary due to secondary Bjerknes force**
- **In the case of uncoated microbubble a formation of a liquid jet in its aft region is observed while the coated one exhibits a deformed shape without permitting extreme elongations**
- **Shape deformations are only exhibited during compressive phase of the pulsation with the microbubble's large axis mainly oriented perpendicularly to the rigid boundary while at the expansion phase the microbubble remains almost spherical**
- **During the compression phase the viscous stresses at the equator are higher than anywhere else and the curvature at this region is decreased in order to satisfy the normal force balance and consequently a prolate shape is favored**

Step change in pressure field: $P_\infty(t) = P_{st} \cdot (1+\varepsilon)$

Coated microbubble (Mooney – Rivlin law, b=0)

$\varepsilon = 2,\ d = 1$

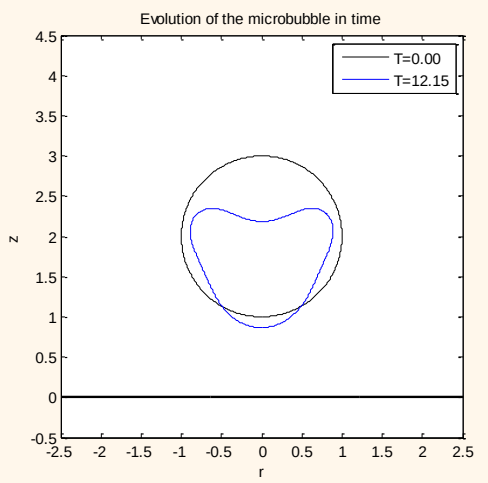

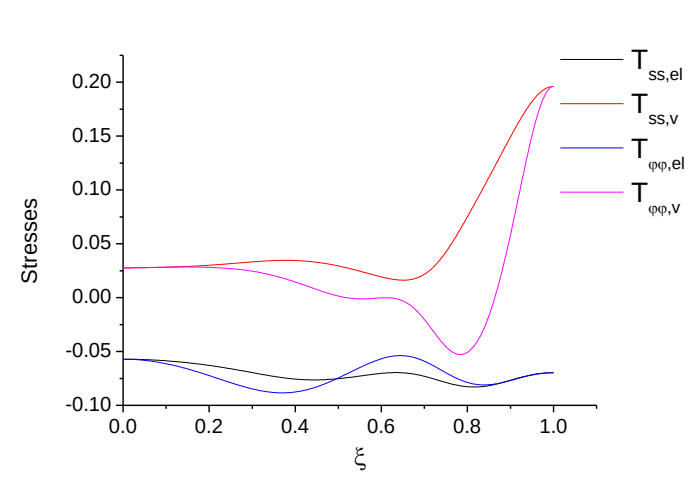

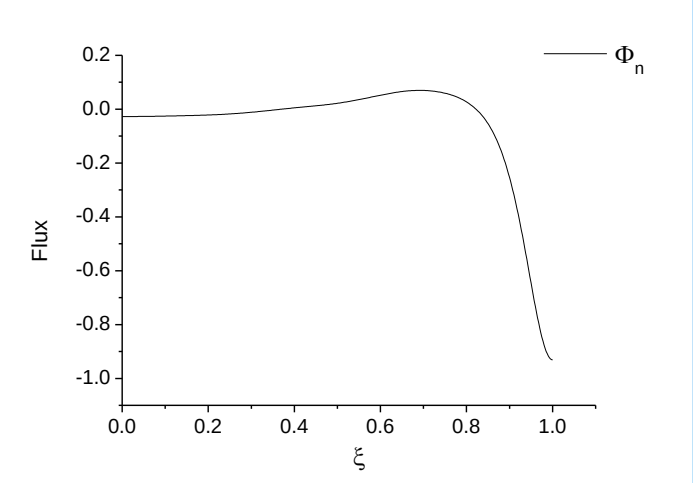

- The upper pole of the microbubble moves very fast toward the opposite side of the bubble causing very high viscous stresses at this region while the pressure at this region is lower than anywhere else on bubble's interface
- At this moment the simulation is terminated. Very high viscous stresses indicate that a shell rupture may occur at this region

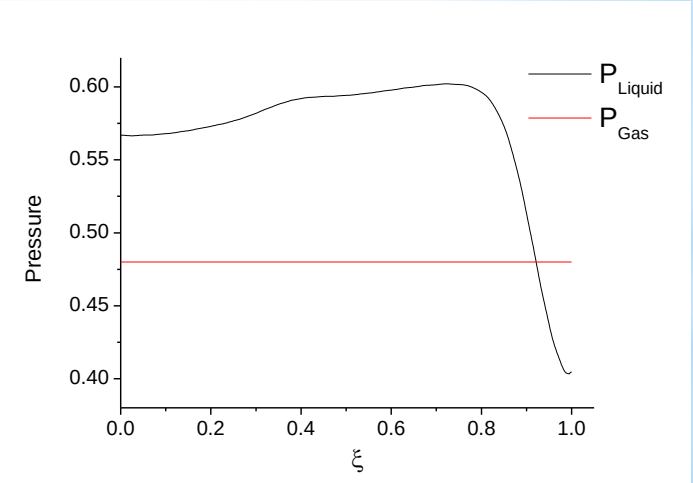

Sinusoidal change in pressure field: $P_\infty(t) = P_{st} \cdot (1 + \varepsilon \cdot \cos t)$

Coated microbubble (Mooney – Rivlin law, b=0)

$\varepsilon = 3,\ d = 1$

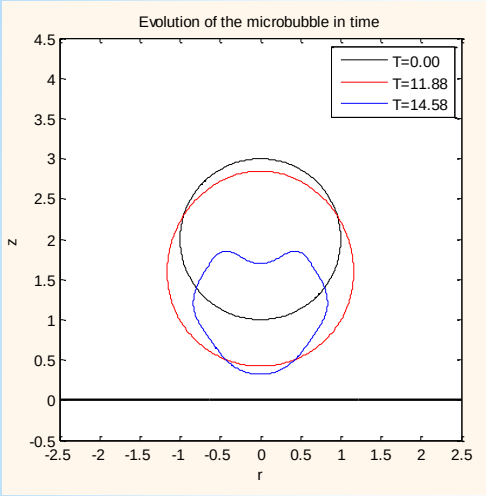

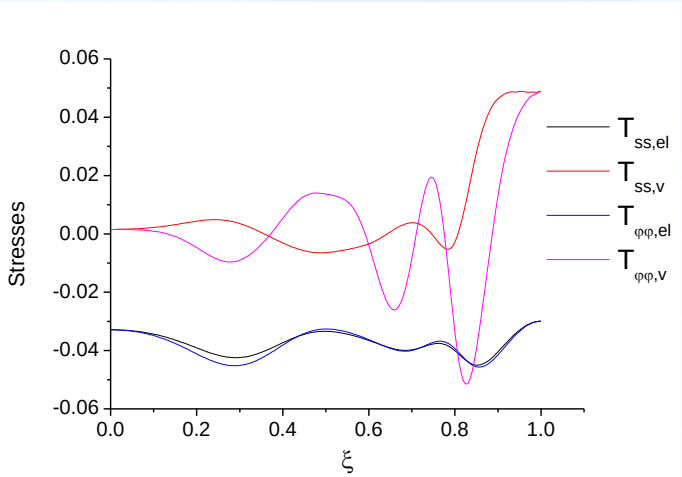

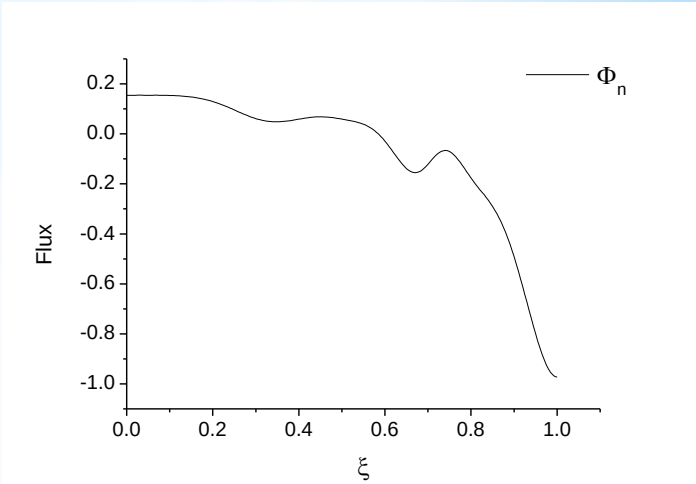

- **Also, in this case, viscous stresses are very large at the upper pole due to its high velocity**
- **The pressure on the interface fluctuates at the aft region of the microbubble where two lobes are formed**
- **The flux at lobes changes its sign indicating that this region tends to be teared apart**

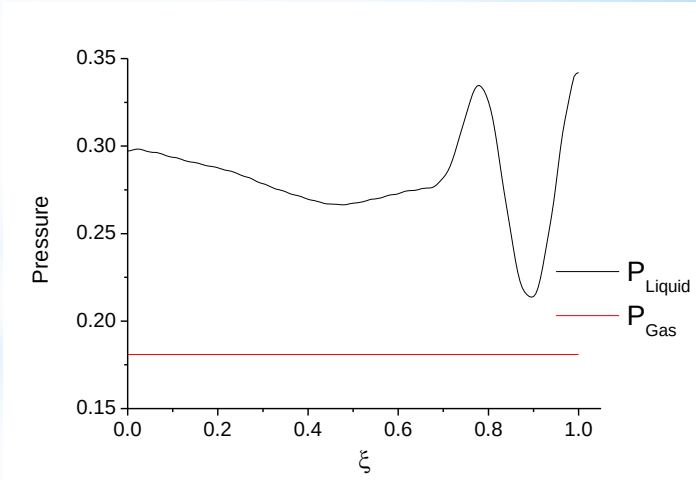

Parametric Study

Coated microbubble (Mooney – Rivlin law, b=0)

Bending modulus: $k_B = 10^{-14}\ \mathrm{N}\cdot m$

Step change: $\varepsilon = 2,\ d = 1$

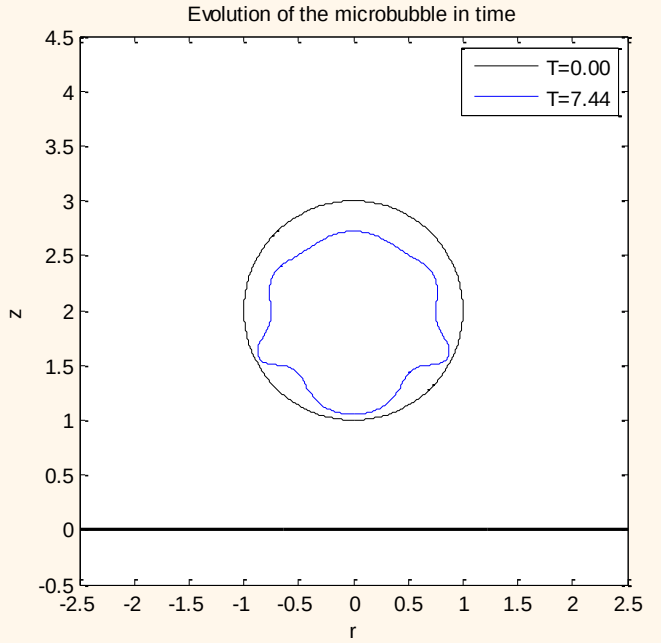

Sinusoidal change: $\varepsilon = 3,\ d = 1$

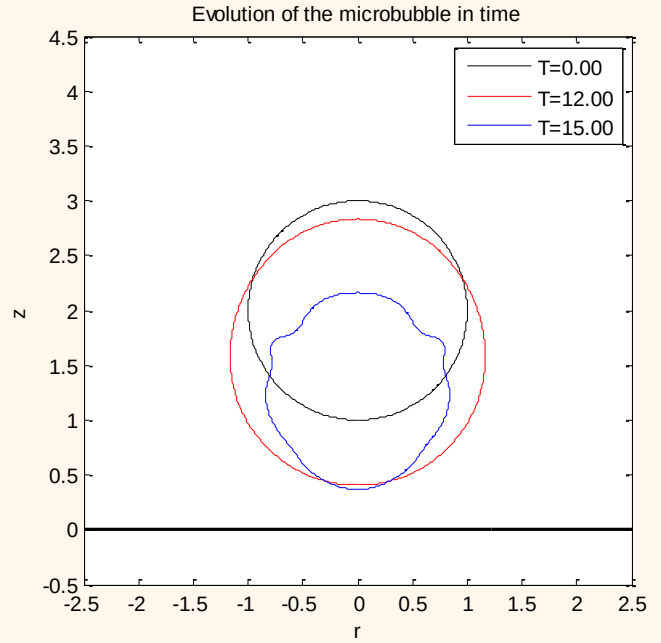

- **In both cases, variation of bending modulus affects the shape mode growth**
- **For lower bending modulus, higher order shape modes are emerging faster via harmonic resonance**
- **Lower bending modulus decreases the bending resistance of the shell causing a multi-lobbed shape deformation**

Parametric Study

Coated microbubble (Skalak law, C=1)

Step change: $\varepsilon = 8,\ \mathrm{d} = 1$

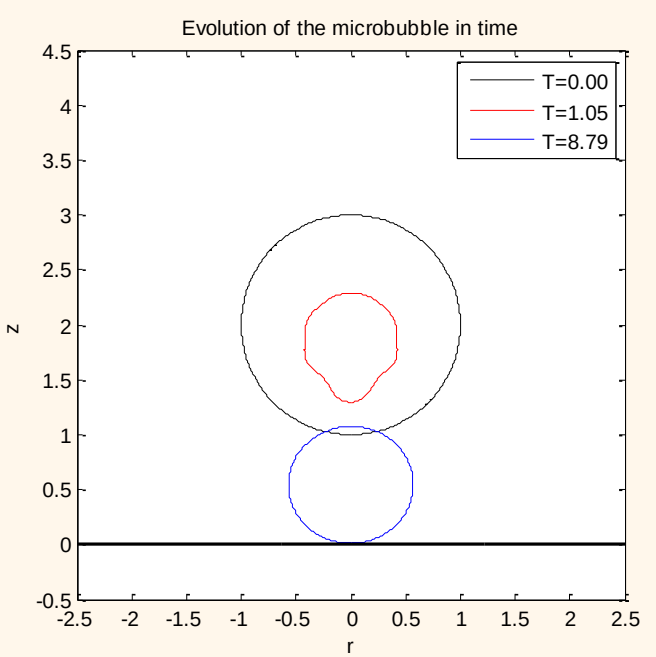

Sinusoidal change: $\varepsilon = 3,\ d = 1$

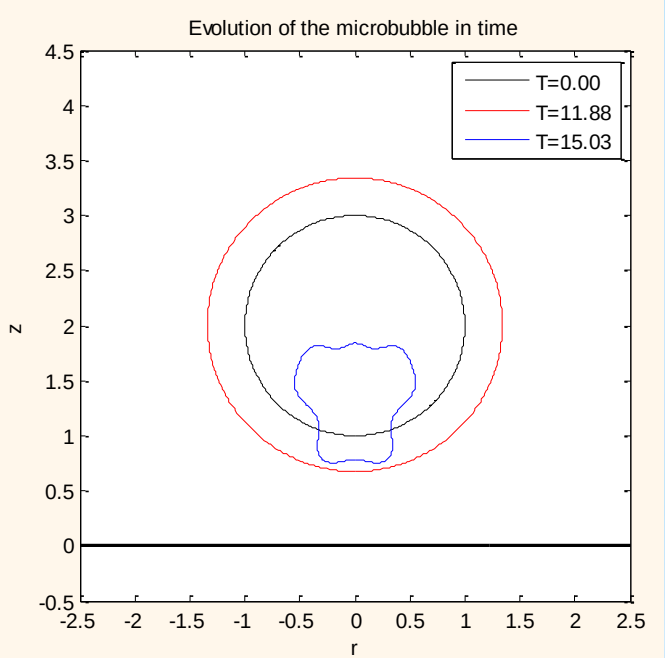

- **Different constitutive law for the shell affects the behavior of the microbubble for both changes of the pressure field**
- **Strain-hardening shells are softened at compression so that, in the case of step change, they can withstand larger pressure loads regaining eventually their spherical shape**
- **For sinusoidal change, the microbubble is deformed along its whole interface during the compression phase while the strain-softening one is deformed mainly in its aft region**

Conclusions

- The microbubble approaches the rigid boundary due to the interaction with the rigid wall (secondary Bjerknes force)
- In the case of uncoated microbubble a formation of a liquid jet in its aft region is observed while in the coated one jet formation is suppressed due to the presence of the viscoelastic shell. Instead, it exhibits a deformed shape without permitting extreme elongations
- For sinusoidal change, shape deformations are only exhibited during compressive phase of the pulsation with the microbubble's large axis mainly oriented perpendicularly to the rigid boundary while at the expansion phase the microbubble remains almost spherical
- During the compression phase the viscous stresses at the equator are higher than anywhere else and the curvature at this region is decreased in order to satisfy the normal force balance and consequently a prolate shape is favored. For lower values of dilatational viscosity a prolate shape is succeeded by an oblate one and vice versa during microbubble's oscillations
- For step change, the uncoated bubble oscillates with its eigenfrequency ω_0 while the oscillations of the coated one are dumped due to dilatational viscosity of the shell and therefore the microbubble keeps propagating due to the absence of viscosity in the surrounding fluid

- For lower bending modulus, higher order shape modes are emerging faster via harmonic resonance due to the decreased bending resistance of the shell
- Strain-hardening shells are softened at compression so that, in the case of step change, they can withstand larger pressure loads regaining eventually their spherical shape. For sinusoidal change, the microbubble is deformed along its whole interface while the strain-softening one is deformed mainly in its aft region

Ongoing & Future work

- Study the interaction between a coated microbubble and a free surface
- Study the interaction between a coated microbubble and an elastic boundary
- Study the dynamic behavior of trapped microbubble
- Development of a numerical model to study the 3D dynamics of a microbubble near a boundary

Acknowledgements

This research has been co-financed by the European Union (European Social Fund - ESF) and Greek national funds through the Operational Program "Education and Lifelong Learning" of the National Strategic Reference Framework (NSRF) - Research Funding Program: Heraclitus II. Investing in knowledge society through the European Social Fund.

Thanks for your attention